Rateless Coding for Hybrid Free-Space Optical and Radio-Frequency Communication

Ali AbdulHussein, Anand Oka, *Member, IEEE*, Trung Thanh Nguyen, *Student Member, IEEE*, and Lutz Lampe, *Senior Member, IEEE*

***Abstract*—Free-space optical (FSO) transmission systems enable high-speed communication with relatively small deployment costs. However, FSO suffers a critical disadvantage, namely susceptibility to fog, smoke, and conditions alike. A possible solution to this dilemma is the use of hybrid systems employing FSO and radio frequency (RF) transmission. In this paper we propose the application of a rateless coded automatic repeat-request scheme for such hybrid FSO/RF systems. The advantages of our approach are (a) the full utilization of available FSO and RF channel resources at any time, regardless of FSO or RF channel conditions and temporal variations, and (b) no need for a-priori rate selection at the transmitter. In order to substantiate these claims, we establish the pertinent capacity limits for hybrid FSO/RF transmission and present simulation results for transmission with off-the-shelf Raptor codes, which achieve realized rates close to these limits under a wide range of channel conditions. We also show that in conditions of strong atmospheric turbulence, rateless coding is advantageous over fixed-rate coding with rate adaptation at the transmitter.**

***Index Terms*—Free-space optical (FSO), hybrid FSO/RF transmission, rateless coding, channel capacity.**

I. Introduction

Free space optical (FSO) communication systems have received renewed interest due to their low deployment costs and potential use in high-throughput applications like last mile access [1]. The main drawback of FSO systems is their limited and unpredictable availability due to atmospheric conditions [2], [3]. To combat the deterioration of signal quality due to adverse atmospheric conditions, various diversity methods have been proposed, including the use of temporal and spatial diversity, e.g. [4]–[7]. However, only media diversity schemes are able to cope with extreme weather conditions like fog or snow which due to scattering cause attenuation of the order of a hundred dB per kilometer. The most prominent media diversity scheme, which retains the above-mentioned advantages of FSO systems, is the use of a license-free radio frequency (RF) channel in conjunction with the FSO channel, e.g., [1]–[3], [8], [9]. The practical heuristic for such hybrid FSO/RF systems is that fog and rain, which drastically affect FSO and RF respectively, but only insignificantly vice versa, rarely occur simultaneously [2], [3].

Commercially available hybrid solutions simply use the RF link as a hot-standby backup for the FSO link, to be used only when the FSO channel is inoperative [1]. Recently, Vangala and Pishro-Nik [8], [9] have presented a coding scheme for the overall hybrid channel based on non-uniform punctured low-density parity check (LDPC) codes. This scheme relies on knowledge of the instantaneous channel conditions at the transmitter and the proper adjustment of code rates for FSO and RF transmission. In this letter, we present an alternative approach to joint FSO/RF channel coding using a practical implementation of rateless Fountain codes [10].[1] Our scheme falls into the class of hybrid automatic repeat-request (HARQ) with incremental redundancy coding [14], and as such does not require rate adjustment *prior* to transmission. This is a clear distinction relative to rate-adaptive coding schemes such as the one proposed in [8], [9]. Our motivation for the application of rateless coding HARQ is twofold. First, it is a very elegant approach for transmission over channels with varying quality such as FSO/RF channels, since it requires neither a bank of codes with various rates nor explicit code selection. Hence, other considerations aside, one may opt for this architecture simply due to its ease of operation. Second, no rate mismatch due to outdated or imprecise channel estimation can occur. This is a distinct performance advantage over schemes with code-rate selection [8], [9], which fail if the channel quality varies notably from one codeword to another. In the context of hybrid FSO/RF systems, these variations may occur especially due to temporal fluctuation in the received optical signal strength due to atmospheric turbulence. HARQ requires reliable feedback from the receiver in the form of negative or positive acknowledgements, and thus the availability of a robust reverse channel for such messages needs to be assumed. We note that this assumption is similar to the feedback requirements for explicit rate adjustment at the transmitter, since the information content of any feedback signal can be made commensurate with the transmitter-side uncertainty about the instantaneous rate supported by the channel.

Manuscript received August 14, 2008; revised July 5 and October 29, 2009. This work was supported by the National Sciences and Engineering Research Council (NSERC) of Canada.

The authors have been with the Deptartment of Electrical and Computer Engineering, University of British Columbia, Vancouver, Canada. Ali AbdulHussein is now with Silvertip Telematics Inc., Vancouver, Canada and Anand Oka is now with Research in Motion, Waterloo, Canada. (e-mail: aabdulhu@gmail.com, anandoka@gmail.com, trungn@ece.ubc.ca, Lampe@ece.ubc.ca).

[1]Parallel to our work, Zhang et al. [11] developed a "soft-switching" scheme for hybrid FSO/RF links using rateless codes similar to ours, with a focus on practical implementation aspects. Also, in course of the review of this letter, references [12], [13] were brought to our attention. They suggest the use of Fountain codes for a parallel multirate FSO transmission method. However, the use of Fountain codes for hybrid FSO/RF systems is not considered in [12], [13].

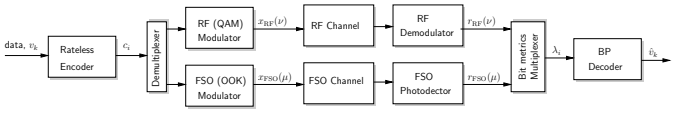

Fig. 1. Block diagram of the proposed coded hybrid FSO/RF transmission system.

It has been proven in [15] that today's most powerful rateless codes, so-called Raptor codes [16], are not universal for channels other than the erasure channel. Hence, a question to be answered is whether there is a single rateless code design that performs *well* for the variety of channel conditions experienced in hybrid FSO/RF channels. This is particularly relevant since FSO and RF channels are characterized by dissimilar transmission statistics. In this letter, we provide evidence that the answer is in the affirmative. To this end, we derive the pertinent modulation-constrained capacity limits for the hybrid FSO/RF channel and show through simulations that a single moderate-length Raptor code design enables us to closely approach these limits under a variety of channel conditions. Our results are in line with the findings in [15], [17], [18] that Raptor codes designed for the binary erasure channel perform remarkably well for binary symmetric and (block-fading) additive white Gaussian noise (AWGN) channels too. Based on the capacity expression we further show that in the strong-turbulence regime, the adjustment of code rate *prior* to transmission will lead to rate loss and codeword outage. Hence, the proposed rateless coding approach provides performance advantages over fixed-rate coding schemes as presented in [8], [9] for hybrid FSO/RF systems.

The remainder of this letter is organized as follows. Section II introduces the transmission model and presents the proposed coding scheme. The pertinent capacity limits are established in Section III, and simulation results for different channel conditions are presented and discussed in Section IV. Section V summarizes the paper.

II. Transmission Model and Proposed Coding Scheme

In this section, we first introduce the channel model and signal schemes used for hybrid FSO/RF transmission and then we describe the proposed coding scheme. The block diagram of the coded hybrid transmission system is shown on Figure 1.

A. Transmission Model

1) Transmitter: The considered hybrid system consists of two transmitter-receiver pairs, one for FSO transmission and one for RF transmission. Both transmitters receive a bit stream from a binary encoder, which is specified in detail in Section II-B. At symbol time index ν, the RF transmitter maps $m_{\mathrm{RF}} = \log_2(M)$ binary symbols to an M-ary quadrature amplitude modulation (M-QAM) signal point $x_{\mathrm{RF}}(\nu)$ using Gray mapping. The QAM constellation is typically non-binary, i.e., $M > 2$, for bandwidth-efficient transmission. The signal elements $x_{\mathrm{RF}}(\nu)$ are sent with a baud rate of $1/T_{\mathrm{RF}}$ symbols per second using conventional pulse shapes such as a root-raised cosine. The FSO transmitter employs intensity modulation with on-off keying (OOK), which is the prevalent modulation format for FSO communication. The signal elements are $x_{\mathrm{FSO}}(\mu) \in \{0, 1\}$ with FSO-symbol-time index μ and the optical signal intensity is P_{FSO} during the on-period and zero during the off-period, each of which is of length T_{FSO}. Obviously, one data bit is represented by one OOK symbol, i.e., $m_{\mathrm{FSO}} = 1$.

2) Channel and Receiver: The FSO receiver applies direct detection. To formulate the transmission model, we adopt the often used photon-count model for direct detection with an ideal photodetector where the μth detector output $r_{\mathrm{FSO}}(\mu)$ has a Poisson count distribution with mean parameter $g_{\mathrm{FSO}}(\mu)K_s + K_b$ if $x_{\mathrm{FSO}}(\mu) = 1$ and K_b if $x_{\mathrm{FSO}}(\mu) = 0$. The constants K_s and K_b are given by $K_s = \eta P_{\mathrm{FSO}} T_{\mathrm{FSO}}/(hf)$ and $K_b = \eta P_b T/(hf)$, where η is the efficiency of the photodetector, f denotes the center frequency of the transmission, h is Planck's constant, and P_b represents the power from background radiation incident on the photodetector [19], [6]. The variable $g_{\mathrm{FSO}}(\mu)$ is the FSO channel gain for the μth transmission.

The RF system uses a line-of-sight link in the millimeter wave band, which is most suitable for a powerful RF back-up with data rates comparable to FSO. The RF receiver consists of a classical matched-filter front-end followed by baud-rate sampling. The sampled and phase-compensated receiver output in the equivalent complex baseband at RF-symbol time ν is written as

$$r_{\mathrm{RF}}(\nu) = g_{\mathrm{RF}}(\nu) x_{\mathrm{RF}}(\nu) + n_{\mathrm{RF}}(\nu)\ , \tag{1}$$

where $g_{\mathrm{RF}}(\nu)$ denotes the real-valued channel gain, $n_{\mathrm{RF}}(\nu)$ is complex-valued AWGN with variance $P_n = \mathcal{N}_0/T_{\mathrm{RF}}$ and $\mathcal{N}_0$ is the one-sided noise power spectral density.

The FSO/RF receiver passes the received samples $r_{\mathrm{FSO}}(\mu)$ and $r_{\mathrm{RF}}(\nu)$ along with the parameters $(g_{\mathrm{FSO}}(\mu)K_s, K_b)$ for the FSO channel, and $(g_{\mathrm{RF}}(\nu), P_n)$ for the RF channel to the bit-metric calculator (see Figure 1).

3) Channel Statistics: The FSO channel gain $g_{\mathrm{FSO}}(\mu)$ includes the effects of signal attenuation and random irradiance fluctuation due to atmospheric turbulence. Signal attenuation is strongly weather dependent and, since weather conditions change very slowly with respect to symbol rate, can safely be assumed to be quasi static. Signal fading due to atmospheric turbulence, i.e., scintillation, occur on a relatively shorter time scale. In this regard, the related literature makes different assumptions about fading rate, ranging from quasi-static to notable temporal changes within a few symbol intervals, cf. e.g. [20]–[22].

It is known, from physical principles, that the optical scintillation process $I(t)$ due to random variations in the refractive index of air is well modeled to be a stationary process with a Gamma-Gamma marginal probability density function (PDF) in all regimes of scintillation (weak to strong). This model results from the observation [23] that $I(t)$ is a multiplication of two independent random processes $I_1(t)$ and $I_2(t)$, corresponding to small and large scale turbulence,

$$I(t) = I_1(t) \cdot I_2(t) \tag{2}$$

and these individual processes are accurately modeled by Gamma marginal PDFs. Similarly, again from physical arguments, the autocovariance function (ACF) $B_1(\tau)$ of $I_1(t)$ and $B_2(\tau)$ of $I_2(t)$ (and hence $B(\tau)$ of $I(t)$) can be derived in a closed form. Both the marginal PDF and the ACF of the small and large scale scintillation are functions of the wavelength λ, the path-length L and the structure parameter C_n^2. In addition, the ACFs also are a function of the wind-speed v. Please refer to [23] for more details.

In this work, we adopt the scintillation model according to (2) with the process $I(t)$ matching the marginal PDF and ACF given in [23, Chapter 3.4]. We note that specifying the marginal PDF and ACF does not uniquely specify the statistical properties of $I(t)$. However, since no reliable expression is known for any higher order statistics, this appears to be the most reasonable approach. Applying sampling at baud rate $1/T_{\mathrm{FSO}}$ we obtain the discrete-time scintillation process $I(\mu)$ and thus the FSO channel gain $g_{\mathrm{FSO}}(\mu)$.

With regards to the millimeter wave RF channel, we observe from e.g. [24] that the gain $g_{\mathrm{RF}}(\nu)$ will remain practically constant for several seconds and thus the assumption of a quasi-static RF channel whose gain does not change during the transmission of (at least) one codeword is validated.

B. Proposed Coding Scheme

1) Encoder and Multiplexing: The hybrid FSO/RF system employs a single encoder of a binary rateless code. More specifically, we apply Raptor codes proposed in [16], whose encoder consists of two stages. The first stage encodes the k-bit input vector $[v_1, v_2, \ldots, v_k]$ into a k'-bit intermediate codevector $[v'_1, v'_2, \ldots, v'_{k'}]$ using a rate-k/k' linear binary block code, for example an LDPC code. In the second stage, a Luby transform (LT) [10] encoder converts the k'-bit LDPC codeword into a semi-infinite stream of Raptor-code bits c_i, $i = 1, 2, \ldots$.

The code bits are then demultiplexed into two bit-streams, one entering the RF QAM modulator and the other one being input to the FSO OOK modulator. To be more specific, let us define the positive, mutually prime integers n_{FSO} and n_{RF} as

$$\frac{n_{\mathrm{FSO}}}{n_{\mathrm{RF}}} = \frac{m_{\mathrm{FSO}}/T_{\mathrm{FSO}}}{m_{\mathrm{RF}}/T_{\mathrm{RF}}} \, . \tag{3}$$

Then, out of a block of $n_{\mathrm{tot}} = n_{\mathrm{FSO}} + n_{\mathrm{RF}}$ bits $[c_i, c_{i+1}, \ldots, c_{i+n_{\mathrm{tot}}-1}]$, the first n_{FSO} bits are passed to the FSO modulator and the remaining n_{RF} bits are RF modulated. The formulation in (3) makes the mild assumption that $m_{\mathrm{FSO}}T_{\mathrm{RF}}/(m_{\mathrm{RF}}T_{\mathrm{FSO}})$ can be expressed as a rational number.

Encoding of the message $[v_1, v_2, \ldots, v_k]$ is terminated when a positive acknowledgment of successful decoding has been received.

2) Metric Computation and Demultiplexing: Based on the received samples and the channel parameters, decoding metrics in the form of log-likelihood ratios are generated.

For FSO transmission with the channel and detector model described in Section II-A the log-likelihood ratio (LLR) associated with $x_{\mathrm{FSO}}(\mu)$ can be written as [25, Eq. (4.5-4)]

$$\lambda_{\mathrm{FSO}}(\mu) = r_{\mathrm{FSO}}(\mu) \log\left(1 + \frac{g_{\mathrm{FSO}}(\mu)K_s}{K_b}\right) - g_{\mathrm{FSO}}(\mu)K_s \, . \tag{4}$$

For RF transmission the LLR for the ℓth bit mapped to $x_{\mathrm{RF}}(\nu)$ is given by (cf. [26, Eq. (7)])

$$\begin{aligned} \lambda^{\ell}_{\mathrm{RF}}(\nu) \;=\; & \log\left[\sum_{x\in\mathcal{X}_{\ell,0}} \exp\left(-\tfrac{|r_{\mathrm{RF}}(\nu)-g_{\mathrm{RF}}(\nu)x|^2}{P_n}\right)\right] \\ & - \log\left[\sum_{x\in\mathcal{X}_{\ell,1}} \exp\left(-\tfrac{|r_{\mathrm{RF}}(\nu)-g_{\mathrm{RF}}(\nu)x|^2}{P_n}\right)\right] \, , \end{aligned} \tag{5}$$

$1 \le \ell \le m_{\mathrm{RF}}$, where $\mathcal{X}_{\ell,b}$ denotes the subset of the QAM signal constellation for which the ℓth bit of the label is equal to $b \in \{0, 1\}$. According to the demultiplexing of code bits described above, groups of n_{FSO} LLRs $\lambda_{\mathrm{FSO}}(\mu)$ and n_{RF} LLRs $\lambda^{\ell}_{\mathrm{RF}}(\nu)$ are multiplexed into one stream of LLRs λ_i, $i = 1, 2, \ldots$, which then is forwarded to the decoder (see Figure 1).

3) Decoder: The decoder for the rateless code collects LLRs λ_i progressively and a first decoding attempt is made when it is believed that sufficient information for successful decoding has been collected. A good estimate for the number n of collected LLRs is given by

$$\sum_{i=1}^{n} C_{\mathrm{H},i} = k(1+\epsilon) \, , \tag{6}$$

where $C_{\mathrm{H},i}$ denotes the constrained capacity of the hybrid FSO/RF channel as defined in Section III below, and $\epsilon > 0$ is an overhead factor which accounts for the suboptimality of the (finite-length) Raptor code with respect to capacity.

Decoding is performed using well-known belief propagation (BP) on the factor graph of the Raptor code. The variable nodes c_i are initialized with the LLRs λ_i, $1 \le i \le n$, and extrinsic likelihood messages are exchanged between the variable and parity-check nodes. If the decoded message $[\hat{v}_1, \hat{v}_2, \ldots, \hat{v}_k]$ after BP decoding is deemed unreliable, which could be determined by either making use of a cyclic redundancy check (CRC) code or estimating the bit-error rate (BER) based on the final LLRs [27], a new decoding attempt is scheduled after a new batch of n_{inc} samples has been received. The value of n_{inc} will depend on the update schedule applied for BP decoding. Complexity-efficient update schedules have been presented in [28], [29].

Once the decoded message $[\hat{v}_1, \hat{v}_2, \ldots, \hat{v}_k]$ is deemed correct, decoding is terminated and an acknowledgment signal is transmitted to the encoder.

4) Remark: We assume that modulation and signalling rate, and thus n_{FSO} and n_{RF} are constant. However, one may opt for adaptive modulation and even adaptive baud rate as a function of the channel conditions. In this case, rateless coding as proposed can still be used in tandem with these to achieve a fine-grained adaptation to the channel conditions (with granularity of n_{inc} bits).

III. Constrained Capacity of the Hybrid FSO/RF Channel

In order to benchmark the proposed coding scheme, we now specify the information-theoretic limit for the hybrid FSO/RF channel. To this end, we first note that the FSO and RF modulation formats are not optimized for maximal mutual information and assumed constant regardless of the channel condition. This is not a particularly limiting assumption since (a) practical FSO use OOK modulation and (b) as long as the size M of the QAM constellation used for RF transmission is chosen such that m_{RF} is at least 1 bit above the Shannon capacity of the RF channel, hardly any gains are achievable with a larger alphabet size [30]. Hence, choosing a reasonably large constellation size, say 64QAM, is sufficiently optimal. Secondly, we note that we are not interested in the ergodic capacity of the hybrid channel due to the typically large coherence times of the RF and FSO scintillation processes (see Section IV-B). Instead, we are interested in the capacity given the sequences of channel gains $[g_{\mathrm{FSO}}(\mu_{\mathrm{s}}),\ldots,g_{\mathrm{FSO}}(\mu_{\mathrm{e}})]$ and $[g_{\mathrm{RF}}(\nu_{\mathrm{s}}),\ldots,g_{\mathrm{RF}}(\nu_{\mathrm{e}})]$ during the transmission of n bits, where $n=(\mu_{\mathrm{e}}-\mu_{\mathrm{s}}+1)m_{\mathrm{FSO}}+(\nu_{\mathrm{e}}-\nu_{\mathrm{s}}+1)m_{\mathrm{RF}}$ and $(\mu_{\mathrm{e}}-\mu_{\mathrm{s}}+1)/(\nu_{\mathrm{e}}-\nu_{\mathrm{s}}+1)=T_{\mathrm{RF}}/T_{\mathrm{FSO}}$.

Let us consider the binary channel from c_i to λ_i (see Figure 1), and denote by μ_i and ν_i the FSO and RF channel symbol-time indices corresponding to the transmission of c_i. Then, since the FSO and RF channels are used in parallel, the constrained hybrid-channel capacity can be written as

$$C_{\mathrm{H},i} = \frac{1}{n_{\mathrm{FSO}}+n_{\mathrm{RF}}}\left[\frac{n_{\mathrm{FSO}}}{m_{\mathrm{FSO}}}C_{\mathrm{FSO}}(g_{\mathrm{FSO}}(\mu_i)) + \frac{n_{\mathrm{RF}}}{m_{\mathrm{RF}}}C_{\mathrm{RF}}(g_{\mathrm{RF}}(\nu_i))\right] \quad (7)$$

with unit [bit/binary channel use], where $C_{\mathrm{FSO}}(g_{\mathrm{FSO}}(\mu))$ and $C_{\mathrm{RF}}(g_{\mathrm{RF}}(\nu))$ respectively denote the constellation-constrained capacities of the FSO and RF channel in bit per FSO and RF channel use for a given channel gain. These are given by (cf. [26, Eq. (14)])

$$C_{\mathrm{FSO}}(g_{\mathrm{FSO}}(\mu)) = 1-\mathbb{E}\left\{\log_2\left[1+\exp\left((-1)^{x_{\mathrm{FSO}}(\mu)}\lambda_{\mathrm{FSO}}(\mu)\right)\right]\right\} \quad (8)$$

$$C_{\mathrm{RF}}(g_{\mathrm{RF}}(\nu)) = m_{\mathrm{RF}}-\sum_{\ell=1}^{m_{\mathrm{RF}}}\mathbb{E}\left\{\log_2\left[1+\exp\left((-1)^{b_\ell}\lambda^{\ell}_{\mathrm{RF}}(\nu)\right)\right]\right\}, \quad (9)$$

where b_ℓ denotes the ℓth bit in the label of $x_{\mathrm{RF}}(\nu)$, and expectation $\mathbb{E}\{\cdot\}$ is with respect to the joint probabilities $p(r_{\mathrm{FSO}}(\mu),x_{\mathrm{FSO}}(\mu))$ and $p(r_{\mathrm{RF}}(\nu),b_\ell)$, respectively. We note that neither $C_{\mathrm{FSO}}(g_{\mathrm{FSO}}(\mu))$ nor $C_{\mathrm{RF}}(g_{\mathrm{RF}}(\nu))$ lend themselves for closed-form expressions, and hence they are evaluated using Monte Carlo integration.

IV. Simulation Results

In this section, we present numerical results and simulative evidence that (a) the proposed coded hybrid FSO/RF scheme performs close to the information-theoretic limits and (b) rateless coded transmission has advantages over fixed-rate schemes with rate selection for hybrid FSO/RF systems.

A. Simulation Setup

1) System Parameters: The considered hybrid system employs 64QAM modulation for RF transmission, i.e., $m_{\mathrm{RF}}=6$, which is practically optimal as long as $C_{\mathrm{RF}}(g_{\mathrm{RF}}(\nu))\leq 5$ bit/(RF channel use) [30]. As specified in Section II-A1, OOK modulation is used for FSO signalling and thus $m_{\mathrm{FSO}}=1$. The FSO baud interval is $T_{\mathrm{FSO}}=10^{-8}$ s and the RF baud interval is adjusted to $T_{\mathrm{RF}}=\frac{m_{\mathrm{RF}}}{m_{\mathrm{FSO}}}T_{\mathrm{FSO}}=6T_{\mathrm{FSO}}$ such that $n_{\mathrm{RF}}=n_{\mathrm{FSO}}=1$ (see Eq. (3)). Furthermore, we assume a wavelength of 1550 nm, a photodetector efficiency of $\eta=0.5$, and a normalized background radiation of $P_bT=-170$ dBJ [6], which yields the average background photon count $K_b=39$. As described in Section II-A3, the RF channel is assumed quasi-static, i.e., $g_{\mathrm{RF}}(\nu)=g_{\mathrm{RF}}$, while the FSO channel gain $g_{\mathrm{FSO}}(\mu)$ varies according to the scintillation process $I(t)$.

For simulations we apply a Raptor code consisting of a rate-0.95 regular LDPC code and an LT code generated using the degree distribution from [16, Table I, 2nd column]. The information word length is chosen as $k=9500$. Decoding is continued until the correct codeword has been found, which emulates the use of a CRC outer code. The number n of code bits required for successful decoding is recorded and the realized rate is obtained as $R=k/n$. The achievable rate according to the capacity limit $C_{\mathrm{H},i}$ in (7) is given by $\bar{R}=k/\bar{n}$, where $\bar{n}$ is defined through

$$\sum_{i=1}^{\bar{n}}C_{\mathrm{H},i}=k\,. \quad (10)$$

The size of decoding increments n_{inc} is set to 0.5% of the expected word length $\bar{n}$ and BP decoding is started afresh after each newly received batch. For termination of transmission after successful decoding, we assume the availability of a reliable feedback channel.

2) A Note on the Generation of the Scintillation Process: Realizations of the scintillation process $I(t)$ are generated by first individually generating $I_1(t)$ and $I_2(t)$ and then using Eq. (2). To match the specified marginal PDFs and ACFs for $I_1(t)$ and $I_2(t)$, the simulated processes are generated by using the randomized Markov chain (MC) algorithm suggested in [31]. The set of transition probabilities of the MC needs to be adjusted (in a one time off-line operation) by solving a non-linear optimization problem to match the ACF. We have used a commercially available non-linear optimization routine which can practically handle up to 16 MC states and found that the resulting solution gave a sufficiently good match for the task at hand.

B. Results and Discussion

First, Figure 2 shows the PDF and ACF of the FSO scintillation process $I(t)$ for an FSO link of $L=1000$ m, a wind-speed of $v=5$ m/s, and different structure parameters C_n^2. The corresponding Rytov variances σ_1^2 and scintillation indices S.I., which are common measures for the strength of irradiance fluctuations, are given in the caption of Figure 2 and represent strong to weak turbulence scenarios, cf. [23]. Also included are the statistics for the simulated process for $C_n^2=10^{-13}$ m$^{-2/3}$. We observe that the channel coherence

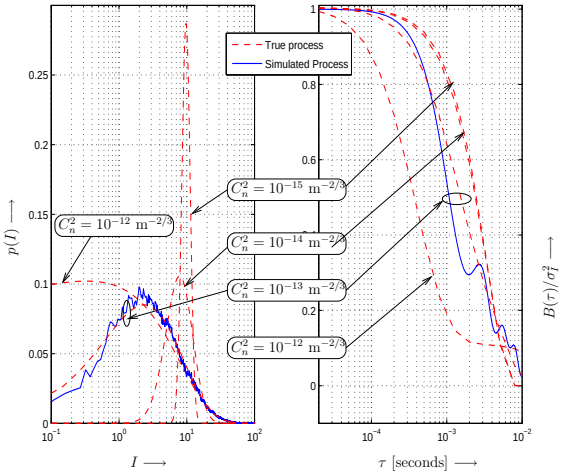

Fig. 2. Statistics of the true gamma-gamma scintillation process $I(t)$, as well as the simulated process, at various values of the structure parameter C_n^2. Left: PDF of I. Right: ACF of $I(t)$ normalized with respect to its variance σ_I^2. Path-length L = 1000 meters, wavelength $\lambda = 1550$ nm, wind-velocity $v = 5.0$ m/s, $\mathbb{E}[I] = 10$. (Rytov variance σ_1^2, scintillation index S.I.) = $\{(19.9, 1.48), (1.99, 0.99), (0.199, 0.173), (0.019, 0.018)\}$ respectively for $C_n^2 = \{10^{-12}, 10^{-13}, 10^{-14}, 10^{-15}\}$ m$^{-2/3}$.

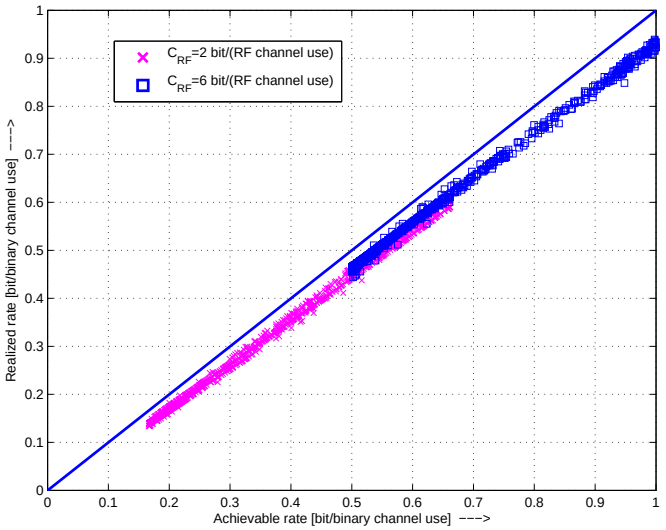

Fig. 3. Scatter plot of realized rate R versus achievable rate $\bar{R}$ according to equation (10). 1000 codewords have been transmitted. FSO channel with $(\sigma_1^2, \text{S.I.}) = (1.99, 0.99)$ and $\mathbb{E}\{C_{\text{FSO}}(g_{\text{FSO}}(\mu))\} = 0.3$ bit/(FSO channel use). Quasi-static RF channel with $C_{\text{RF}} = \{2.0, 6.0\}$ bit/(RF channel use).

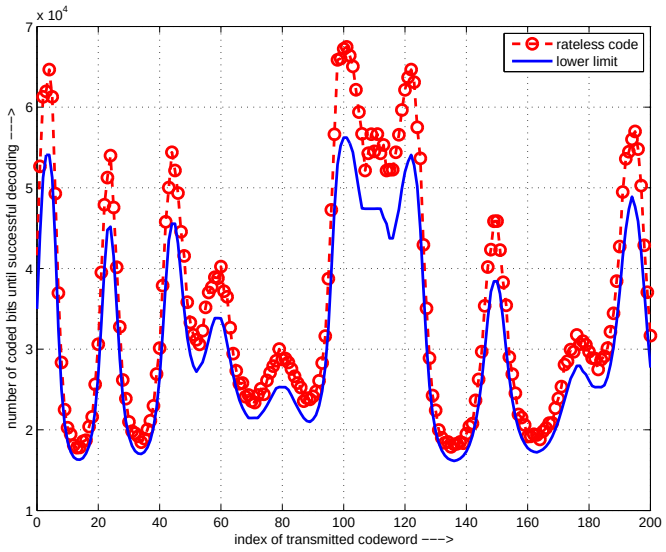

Fig. 4. Number of transmitted coded bits until successful decoding for 200 codeword transmissions. Simulated codeword length n using rateless codes and lower limit $\bar{n}$ from equation (10). FSO channel with $(\sigma_1^2, \text{S.I.}) = (1.99, 0.99)$ and $\mathbb{E}\{C_{\text{FSO}}(g_{\text{FSO}}(\mu))\} = 0.3$ bit/(FSO channel use). Quasi-static RF channel with $C_{\text{RF}} = 2.0$ bit/(RF channel use).

time is on the order of milliseconds and decreases for relatively strong turbulence scenarios. More significant though are the differences in the PDF, which indicates the occurrence of deep fades in the strong turbulence regime. It can further be seen that the statistics of the simulated process are a good match to the true statistics. For the following performance results we assume the above parameters L and v, and that $C_n^2 = 10^{-13}$ m$^{-2/3}$ and thus relatively strong turbulence with $(\sigma_1^2, \text{S.I.}) = (1.99, 0.99)$.

Figure 3 compares the rate R achieved with rateless coding and the achievable rate $\bar{R}$ according to equation (10) for the hybrid FSO/RF system and 1000 transmitted codewords. The FSO channel supports an average rate of $\mathbb{E}\{C_{\text{FSO}}(g_{\text{FSO}}(\mu))\} = 0.3$ bit/(FSO channel use), while the quasi-static RF channel gain is adjusted such that $C_{\text{RF}} = \{2.0, 6.0\}$ bit/(RF channel use). We observe that the rateless coded system performs consistently close to the capacity limit, regardless of the instantaneous FSO or RF channel gains and thus achievable rate. In particular, the overhead ϵ (see (6)) remains between about 10-20 % in all cases and thus, the same rateless code design performs well for very different mixtures and qualities of FSO and RF channels. We also observe the boost in realized and achievable rate due to a stronger RF channel, which will be further elaborated below.

The ability of the rateless coding scheme to adapt the instantaneous channel conditions is further highlighted in Figure 4, which shows for 200 transmitted codewords that the required codeword length n follows the lower limit $\bar{n}$ from equation (10). The results in Figures 3 and 4 clearly support the idea of rateless coding to achieve close-to-capacity performance in hybrid FSO/RF systems. In particular, the use of a single degree distribution, taken from [16, Table I, 2nd column], is justified by the consistency with which the capacity limit is approached. Similar observations have been made in [13, 14] for transmission over AWGN channels. This renders rateless coding a very attractive approach as no adjustment of the code structure is necessary.

The effect of the RF back-up, used concurrently with the FSO link operating in strong turbulence conditions, is illustrated in Figure 5, where we plot the measured complementary cumulative density function (CCDF) of $\bar{n}$ for $k = 9500$ and RF channels with different capacities. It can be seen that the scintillation process $I(t)$ and the resulting variation of $g_{\text{FSO}}(\mu)$ leads to large fluctuations of $\bar{n}$, which in turn makes the achievable throughput a random variable. The integration

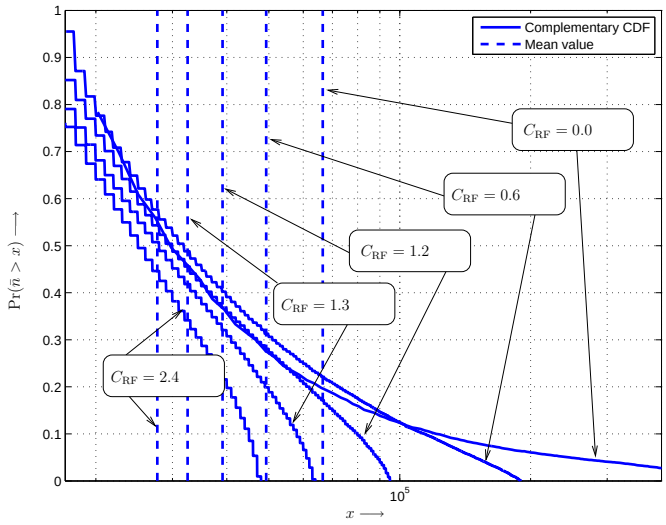

Fig. 5. Complementary CDF of $\bar{n}$ from equation (10) with $k = 9500$ for various values of $C_{\rm RF}$ (unit is bit/(RF channel use)). FSO channel with $(\sigma_1^2, \text{S.I.}) = (1.99, 0.99)$ and $\mathbb{E}\{C_{\rm FSO}(g_{\rm FSO}(\mu))\} = 0.3$ bit/(FSO channel use).

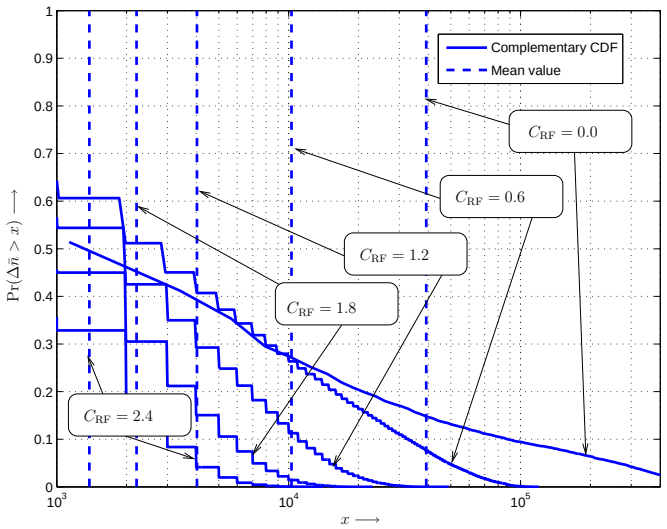

Fig. 6. Complementary CDF of the successive difference $\Delta\bar{n}$ of $\bar{n}$ from equation (10) with $k = 9500$ for various values of $C_{\rm RF}$ (unit is bit/(RF channel use)). FSO channel with $(\sigma_1^2, \text{S.I.}) = (1.99, 0.99)$ and $\mathbb{E}\{C_{\rm FSO}(g_{\rm FSO}(\mu))\} = 0.3$ bit/(FSO channel use).

of the RF channel through joint coding moderates ('dampens') the throughput fluctuations, with more pronounced effect for large RF channel capacity. In particular, in accordance with information theory, the mean of the distribution does decrease monotonically as the RF capacity increases. The observation that the curve for $C_{\rm RF} = 0$ intersects with curves for $C_{\rm RF} > 0$ is not a contradiction, but reflects the larger variance of the required number of received samples $\bar{n}$ for smaller $C_{\rm RF}$.

Finally, it is interesting to consider the change in required codeword length, and thus code rate, for *successively* transmitted codewords. For this purpose, Figure 6 plots the CCDF of $\Delta\bar{n}$, which is the difference of two successive values of $\bar{n}$, for $k = 9500$ and RF channels with different capacities. We observe that notable variations in required codeword length from one codeword to the next occur with high probability, especially when $C_{\rm RF}$ is low. This implies that coding schemes using fixed-rate codes with a-priori rate adjustment based on the prior received word, as in [8], [9], will be affected by a significant rate mismatch. That is, either a rate loss is suffered or outages occur. In contrast, as confirmed by our simulations, the proposed rateless coded system is able to seamlessly adapt to these changes. To provide one concrete, quantitative example, we consider a fixed-rate coding scheme for the scenario with $C_{\rm RF} = 1.2$ bit/(RF channel use) from Figures 5 and 6. The code rate for the ith codeword is chosen as $R_i = (1 + \Delta)k/\bar{n}_{i-1}$, where $\bar{n}_{i-1}$ is the achievable rate from (10) for the transmission of the $(i-1)$st codeword. That is, the receiver provides the transmitter with most up-to-date channel information before transmission. Δ is a margin to account for channel variations. Then, even when assuming that a decoding error occurs only if $R_i > k/\bar{n}_i$ (which is a highly optimistical assumption for this scheme), we obtain outage rates of 17% for $\Delta = 10\%$ and 7% for $\Delta = 20\%$. We can thus conclude that the rateless coding scheme is not only an elegant approach to utilize resources in hybrid FSO/RF systems, but also enjoys a distinct throughput advantage over coding with a-priori rate selection in strong turbulence situations.

V. Conclusions

We have proposed the application of rateless codes for hybrid FSO/RF transmission systems. Hybrid FSO/RF systems combine the best of two worlds to render the system performance robust to short and long-term variations of the FSO and RF transmission channel. This is critical for the adoption of FSO as a reliable high-speed access technology. The distinct feature of the proposed scheme is that it (a) enables the realization of the potential advantages due to parallel FSO and RF channels without the need for redesign or reconfiguration of the transmitter-side coding or modulation and (b) adapts seamlessly to the changes in rate supported by the channel. We have established the pertinent information-theoretic limits, which show that coding schemes with transmitter side rate selection may suffer from rate loss or outages depending on the rate of channel fluctuation. Simulative evidence has been provided that the proposed rateless coding scheme, using an off-the-shelf Raptor code, well approaches the information-theoretic limits regardless of channel conditions.

References

[1] S. Bloom and W. Hartley, "The last-mile solution: Hybrid FSO radio," in *Whitepaper, AirFiber Inc.*, May 2002.

[2] I. I. Kim and E. Korevaar, "Availability of free space optics (FSO) and hybrid FSO/RF systems," in *Proc. SPIE, Optical Wireless Communications IV*, vol. 4530, Denver, CO, USA, Aug. 2001, pp. 84–95.

[3] J. Pan, M. Evans, T. Euler, H. Johnson, and F. DeNap, "Free-space optical communications: Opportunities and challenges, a carrier's perspective," in *Proc. SPIE, Wireless and Mobile Communications II*, vol. 4911, 2002, pp. 58–72.

[4] V. Chan, "Coding for the turbulent atmospheric optical channel," *IEEE Trans. Commun.*, vol. 30, pp. 269–275, Jan. 1982.

[5] E. Lee and V. Chan, "Optical communication over the clear turbulent atmospheric channel using diversity," *IEEE J. Select. Areas Commun.*, vol. 22, pp. 1896–1906, Nov. 2004.

[6] S. Wilson, M. Brandt-Pearce, Q. Cao, and J. Leveque, III, "Free-space optical MIMO transmission with Q-ary PPM," *IEEE Trans. Commun.*, vol. 53, no. 8, pp. 1402 – 1412, Aug. 2005.

[7] M. Safari and M. Uysal, "Do we really need OSTBCs for free-space optical communication with direct detection?" *IEEE Trans. Wireless Commun.*, vol. 7, no. 11, pp. 4445–4448, November 2008.

[8] S. Vangala and H. Pishro-Nik, "Optimal hybrid RF-wireless optical communication for maximum efficiency and reliability," in *Proc. 41st Annual Conference on Information Sciences and Systems (CISS)*, Mar. 2007, pp. 684–689.

[9] ——, "A highly reliable FSO/RF communication system using efficient codes," in *Proc. IEEE Global Telecommunications Conference (GLOBECOM)*, Washington, DC, USA, Nov. 2007, pp. 2232–2236.

[10] M. Luby, "LT codes," in *IEEE Symp. on Foundations of Comp. Sc. (FOCS)*, Vancouver, BC, Canada, Nov. 2002, pp. 271–280.

[11] W. Zhang, S. Hranilovic, and C. Chi, "Soft-switching hybrid FSO/RF links using short-length raptor codes: Design and implementation," *IEEE J. Select. Areas Commun.*, vol. 27, no. 9, pp. 1698–1708, Dec. 2009.

[12] S. Navidpour, B. Hamzeh, and M. Kavehrad, "Multirate fractal free space optical communications using Fountain codes," in *Proc. SPIE, Optical Transm. Syst. and Equipm,. for WDM Netw.*, vol. 6012, 2005, pp. U1–U7.

[13] M. Kavehrad, S. Navidpour, and S. Lee, "Fractal transmission in a hybrid RF and wireless optical link; a reliable way to beam bandwidth in a 3D-global grid," in *Proc. SPIE, Broadband Access Commun. Techn.*, vol. 6390, 2006, pp. E1–E11.

[14] C. Lott, O. Milenkovic, and E. Soljanin, "Hybrid ARQ: Theory, state of the art and future directions," *IEEE Information Theory Workshop on Information Theory for Wireless Networks*, pp. 1–5, July 2007.

[15] O. Etesami and A. Shokrollahi, "Raptor codes on binary memoryless symmetric channels," *IEEE Trans. Inform. Theory*, vol. 52, no. 5, pp. 2033 – 2051, May 2006.

[16] A. Shokrollahi, "Raptor codes," *IEEE Trans. Inform. Theory*, vol. 52, no. 6, pp. 2551 – 2567, Jun. 2006.

[17] R. Palanki and J. Yedidia, "Rateless codes on noisy channels," in *Proc. IEEE International Symposium on Information Theory (ISIT)*, Chicago, IL, USA, June-July 2004, p. 37, (see also www.merl.com/papers/TR2003-124/).

[18] J. Castura and Y. Mao, "Rateless coding over fading channels," *IEEE Commun. Lett.*, vol. 10, no. 1, pp. 46–48, Jan. 2006.

[19] R. Gagliardi and S. Karp, *Optical Communications*. New York: John Wiley & Sons, 1976.

[20] H. Henniger, F. David, D. Giggenbach, and C. Rapp, "Evaluation of FEC for the atmposheric optical IM/DD channel," in *Proc. SPIE, Free-Space Laser Communications XV*, vol. 4975, 2003, pp. 1–11.

[21] X. Zhu, J. Kahn, and J. Wang, "Mitigation of turbulence-induced scintillation noise in free-space optical links using temporal-domain detection techniques," *IEEE Photon. Technol. Lett.*, vol. 15, no. 4, pp. 623–625, April 2003.

[22] M. Uysal, S. Navidpour, and J. Li, "Error rate performance of coded free-space optical links over strong turbulence channels," *IEEE Commun. Lett.*, vol. 8, no. 10, pp. 635–637, Oct. 2004.

[23] L. Andrews, R. Phillips, and C. Hopen, *Laser Beam Scintillation with Applications*. Bellingham, WA: SPIE Press, 2001.

[24] F. Medeiros Filho, D. Jayasuriya, R. Cole, and C. Helmis, "Spectral density of millimeter wave amplitude scintillations in an absorption region," *IEEE Trans. Antennas Propagat.*, vol. 31, no. 4, pp. 672–676, Jul 1983.

[25] S. Dolinar, J. Hamkins, B. Moision, and V. Vilnrotter, "Optical modulation and coding," in *Deep Space Optical Communications*, H. Hemmati, Ed. Wiley-Interscience, Apr. 2006.

[26] G. Caire, G. Taricco, and E. Biglieri, "Bit-interleaved coded modulation," *IEEE Trans. Inform. Theory*, vol. 44, no. 3, pp. 927–946, May 1998.

[27] P. Hoeher, "Adaptive modulation and channel coding using reliability information," in *Proc. of 5th International OFDM-Workshop*, Hamburg, Germany, Sep. 2000, pp. 14.1–14.4.

[28] K. Hu, J. Castura, and Y. Mao, "Performance-complexity tradeoffs of Raptor codes over Gaussian channels," *IEEE Commun. Lett.*, vol. 11, no. 4, pp. 343 – 345, Apr. 2007.

[29] A. AbdulHussein, A. Oka, and L. Lampe, "Decoding with early termination for Raptor codes," *IEEE Commun. Lett.*, vol. 12, no. 6, pp. 444 – 446, Jun. 2008.

[30] L. Ozarow and A. Wyner, "On the capacity of the Gaussian channel with a finite number of input levels," *IEEE Trans. Inform. Theory*, vol. 36, no. 11, pp. 1426–1428, Nov. 1990.

[31] A. S. Rodionov, H. Choo, H. Y. Youn, and T. M. Chung, "Generation of Pseudo Random Processes with a Given Marginal Distribution and Autocorrelation Function," *Intl. Journal of Computer Mathematics*, vol. 78, no. 4, pp. 521–537, Jan. 2001.